

## Original Article

# miRNA-9 expression is upregulated in the spinal cord of G93A-SOD1 transgenic mice

Fenghua Zhou<sup>1</sup>, Yingjun Guan<sup>2</sup>, Yanchun Chen<sup>2</sup>, Caixia Zhang<sup>2</sup>, Li Yu<sup>2</sup>, Hailing Gao<sup>2</sup>, Hongmei Du<sup>2</sup>, Bing Liu<sup>2</sup>, Xin Wang<sup>3</sup>

<sup>1</sup>Department of Pathology, Weifang Medical University, Weifang, Shandong, P. R. China; <sup>2</sup>Department of Histology and Embryology, Weifang Medical University, Weifang, Shandong, P. R. China; <sup>3</sup>Department of Neurosurgery, Brigham and Women's Hospital, Harvard Medical School, Boston, MA, USA

Received June 29, 2013; Accepted August 3, 2013; Epub August 15, 2013; Published September 1, 2013

**Abstract:** The pathogenesis of amyotrophic lateral sclerosis (ALS) remains unclear. Accumulating evidence indicates that various miRNAs expressed in a spatially and temporally controlled manner in the nervous system have an important function in the development of neurodegenerative diseases. The present study aimed to determine the expression and cellular distribution of miRNA-9 in the spinal cord of G93A-SOD1 mutant mice at different time points (post-natal 95, 108 and 122 d). miRNA expression was evaluated by microarray analysis; differentially expressed miRNAs were validated by RT-qPCR. The cellular distribution of miRNA-9 was analyzed by in-situ hybridization. Microarray results indicated for the first time that various miRNAs were differentially expressed between the G93A-SOD1 mutant mice and the littermate control mice. miRNA-9 expression was upregulated at 95, 108, and 122 d as validated by microarray analysis, RT-qPCR, and ISH. ISH results also showed that the miRNA-9-positive cells mainly expressed in the cytoplasm were located in the dorsal horn and the ventral horn of the spinal cord. The majority of miRNA-9-positive cells were located in the ventral horn of the gray matter, the locus of neurodegeneration. These results indicated that the differential expression of miRNA-9 may have an important function in the pathogenesis of G93A-SOD1 transgenic mice.

**Keywords:** ALS, miRNA-9, differential expression

## Introduction

Amyotrophic lateral sclerosis (ALS) is an adult-onset neurodegenerative disorder, which is characterized by the progressive and selective loss of motor neurons in the cerebral cortex, the brainstem, and the spinal cord [1, 2]. However, effective treatments to reduce motor neuron degeneration are not yet available [3]. Sporadic (no family history) and genetic (inherited) forms of ALS have been reported. The majority of ALS cases are sporadic (SALS), and approximately 5 to 10% are familial (FALS). Mutations in the superoxide mutase 1 (SOD1) gene represent one of the most commonly identified causes of FALS, accounting for approximately 20% of the cases [4]. To date, the pathogenesis of ALS remains largely unknown.

microRNAs (miRNAs) are short (approximately 22 nucleotides in length), highly conserved,

and single-stranded RNA molecules that regulate gene expression by either promoting the degradation or inhibiting the translation of target mRNAs [5]. miRNAs are involved in various physiological and pathological processes, such as tumorigenesis [1, 6]. Studies [7-9] have demonstrated that miRNAs are associated with the development of the central nervous system and the pathogenesis of neurodegenerative diseases. However, few studies on miRNAs in ALS have been conducted. In the present study, the differential expression of miRNAs and the distribution of miRNA-9 in the spinal cord of G93A-SOD1 transgenic mice were investigated.

## Materials and methods

### *Animals and tissues*

Transgenic mice were purchased from Jackson Laboratories (Bar Harbor, ME, USA). The mice

express a low copy number of a mutant form of superoxide dismutase (SOD1) with glycine-93 replaced with alanine (G93A-SOD1), which can mimic the progression of human ALS symptoms. The mice in this study were housed under standard conditions: a constant temperature of  $22 \pm 1$  °C; 40% relative humidity; 12 h / 12 h light/dark cycle; and free access to food and water. The mice were crossbred and PCR genotyping was performed using genomic DNA from the tails of newborn mice according to the genotyping protocol of Jackson Laboratory [10]. The Animal Ethics Committee of Weifang Medical University approved the experimental protocols. The mice were then divided in two groups: G93A-SOD1 transgenic and wild-type groups. The wild-type group was used as the control group. The mice from each group were sacrificed at early (95 d), middle (108 d), and late (122 d) stages. Spinal cord samples were collected immediately. Some of the samples were stored in liquid nitrogen for microarray analysis and RT-qPCR. The other samples were perfused intracardially with 4% paraformaldehyde in 0.1 M phosphate buffer and fixed in 4% paraformaldehyde for in-situ hybridization analysis.

#### *Detection of miRNA expression*

Exiqon miRCURY™ LNA array v.18.0 containing approximately 1200 capture probes and covering all of the mouse miRNAs was used to quantify genome-wide miRNA expression in the two groups. Each sample (1 µg) was 3-end-labeled with Hy3™ fluorescent labeling kit (Exiqon, Vedbaek) and hybridized on LNA arrays according to the manufacturer's instructions. The slides were then scanned using Axon GenePix 4000B microarray scanner. The scanned images were imported in GenePix Pro 6.0 software (Axon) for grid alignment and data extraction. The replicated miRNAs were averaged and the miRNAs with intensities  $\geq 30$  in all of the samples were chosen to calculate the normalization factor. The differentially expressed miRNAs were identified by fold change filtering. Hierarchical clustering was performed to identify the distinguishable miRNA expression profiling among the samples by using MEV software (v4.6, TIGR).

#### *RNA isolation and cDNA synthesis*

RT-qPCR was performed to validate the microarray results. Total RNA was isolated from the spinal cord derived from G93A-SOD1 and wild-

type mice by using Trizol reagent (Invitrogen) according to the manufacturer's protocol. The amount of RNA was quantified using an ND-1000 spectrophotometer (Nano-drop). RNA quality was verified by measuring the OD260/OD280 ratio. The total RNA (1 µg) was reverse transcribed to produce cDNA by using M-MLV transcriptase (Promega). The following primers were used in reverse transcription: (miRNA-9), 5'-GTCGTATCCAGTGC GTGTCGTGGAGTCGGCA-ATTGCACTGGATACGACTCATACA-3'; (U6), 5'-CGCTTCACGAATTTGCGTGCAT-3'. The SuperScript III cDNA synthesis reaction was diluted at a ratio of 1:2 by using sterile water for RT-qPCR.

#### *RT-qPCR*

Each qPCR was performed for miRNA-9 and U6 in a final volume of 20 µl. Endogenous U6 expression was used as the control treatment. The reaction system comprised different components. For miRNA-9, the following substances were used: 10 µl of 2× SoFast TMEva Green Supermix mix (BIO-RAD, Singapore); 1 µl of miRNA-9 primer assay; 4 µl of diluted cDNA, and 4 µl of sterile water. For U6, the following materials were used: 10 µl of 2× SoFast TMEvaGreen Supermix mix (BIO-RAD); 0.5 µl of U6 primer assay; 4 µl of diluted cDNA; and 5 µl of sterile water. The following primers were used in qPCR: (miRNA-9) sense, 5'-GGGTCTTTGGTTATCTAGC-3'; antisense, 5'-TGC GTGTCGTG-GAGTC-3'; (U6) sense, 5'-GCTTCGGCAGCACATATACTAAAAT-3'; and antisense, 5'-CGCTTCACGAATTTGCGTGCAT-3'. Amplification was performed using the following program cycle: initial melting temperature, 95 °C for 5 min followed by 40 cycles of 95 °C for 5 s; 60 °C for 30 s; 72 °C for 30 s; and 80 °C for 10 s. Each cDNA sample was analyzed in triplicate. The difference in the relative expression of miRNA-9 between ALS and wild-type mice was calculated using the  $2^{-\Delta\Delta Ct}$  method.

#### *In situ hybridization*

5-DIG labeled miRCURY LNA™ detection probe (Product no. 88078-01, sequence: TCATACAGC-TAGATAACCAAAGA, Exiqon) was used for ISH to detect the miRNA-9 expression in the spinal cord. The samples were perfused intracardially with 4% paraformaldehyde in 0.1 M phosphate buffer and fixed in 4% paraformaldehyde overnight at 4 °C. The samples were then dehydrated in 30% sucrose/PB O/N at 4 °C and cut into 10 µm sections from OCT embedded FrFr

## miRNAs and miRNA-9 in ALS

**Table 1.** miRNAs upregulated by more than twofold at 95 d

Name	Fold change	Name	Fold change	Name	Fold change
mmu-miR-137-5p	2.452403	mmu-miR-532-5p	2.289189	mmu-miR-3970	2.793397
mmu-miR-695	2.783668	mmu-miR-1958	2.371464	mmu-let-7a-5p	3.236796
mmu-miR-10a-5p	2.111037	mmu-miR-33-5p	2.27027	mmu-miR-21a-5p	2.38365
mmu-miR-330-5p	2.085822	mmu-miR-92a-2-5p	2.601351	mmu-miR-488-3p	2.043919
mmu-miR-872-5p	2.008821	mmu-miR-107-3p	2.135071	mmu-miR-181b-5p	2.834276
mmu-miR-1953	5.809685	mmu-miR-1892	2.21982	mmu-miR-145a-5p	2.208494
mmu-miR-30a-5p	2.00104	mmu-miR-9-5p	2.18264	mmu-miR-323-3p	2.132593
mmu-miR-541-3p	2.531624	mmu-miR-137-3p	2.160253	mmu-miR-338-3p	3.961199
mmu-miR-5115	2.591717	mmu-miR-344b-3p	2.579673	mmu-miR-3068-3p	2.391892
mmu-miR-679-5p	2.714137	mmu-miR-219-5p	5.587106	mmu-miR-346-5p	2.65124
mmu-miR-136-5p	2.135088	mmu-miR-770-3p	2.01685	mmu-miR-214-3p	3.488871
mmu-miR-29b-3p	3.202007	mmu-miR-29c-3p	3.104722	mmu-miR-701-5p	2.211149
mmu-miR-5105	2.055702	mmu-miR-29a-3p	2.744773	mmu-miR-28a-5p	2.307286
mmu-miR-128-3p	2.706465	mmu-let-7f-5p	4.536757	mmu-miR-758-5p	3.254054
mmu-miR-883b-5p	2.334371	mmu-miR-18a-3p	2.041815	mmu-miR-380-3p	2.220855

**Table 2.** miRNAs downregulated by more than twofold at 95 d

Name	Fold change	Name	Fold change	Name	Fold change
mmu-miR-27b-3p	0.476114	mmu-miR-193a-3p	0.279701	mmu-miR-3069-3p	0.384301
mmu-miR-146b-5p	0.428458	mmu-miR-186-5p	0.275878	mmu-miR-433-3p	0.196247
mmu-miR-487b-3p	0.478313	mmu-miR-337-3p	0.313496	mmu-miR-1843a-5p	0.415933
mmu-miR-340-5p	0.351139	mmu-miR-25-5p	0.325169	mmu-miR-127-5p	0.246626
mmu-miR-34c-5p	0.44376	mmu-miR-543-3p	0.176221	mmu-miR-106b-5p	0.336679
mmu-miR-139-5p	0.438943	mmu-miR-411-3p	0.208108	mmu-miR-96-5p	0.361927
mmu-miR-382-5p	0.279887	mmu-miR-3096a-3p	0.228304	mmu-miR-7a-5p	0.273277
mmu-miR-1843a-3p	0.412089	mmu-miR-466a-3p	0.49247	mmu-miR-466a-3p	0.404655
mmu-miR-29b-1-5p	0.419107	mmu-miR-34b-5p	0.300033	mmu-miR-331-3p	0.226319
mmu-miR-182-5p	0.138739	mmu-miR-434-5p	0.33917	mmu-miR-190a-3p	0.443964
mmu-miR-210-3p	0.232322	mmu-miR-99b-5p	0.175193	mmu-miR-3096a-5p	0.409574
mmu-miR-132-5p	0.371622	mmu-miR-495-3p	0.288044	mmu-miR-30c-1-3p	0.471495
mmu-miR-3094-3p	0.416216	mmu-miR-379-5p	0.226204	mmu-miR-34a-5p	0.416461
mmu-miR-342-5p	0.180964	mmu-miR-153-3p	0.256331	mmu-miR-455-3p	0.251744
mmu-miR-154-3p	0.452409	mmu-miR-129-5p	0.156382	mmu-miR-873a-5p	0.433559
mmu-miR-190a-5p	0.354376	mmu-miR-344-3p	0.346847	mmu-miR-1839-3p	0.283954
mmu-miR-674-5p	0.203119	mmu-miR-3069-5p	0.244422	mmu-miR-3475	0.488254
mmu-miR-212-3p	0.406146	mmu-miR-222-3p	0.178797	mmu-miR-339-5p	0.257378
mmu-miR-423-3p	0.46661	mmu-miR-3962	0.450364	mmu-miR-125b-2-3p	0.353998
mmu-miR-338-5p	0.342989	mmu-miR-1843b-5p	0.201995	mmu-miR-10b-3p	0.405634
mmu-miR-212-5p	0.383357	mmu-miR-219-2-3p	0.424644	mmu-miR-185-5p	0.223381
mmu-miR-467b-5p	0.360187	mmu-miR-125a-3p	0.431444	mmu-miR-146a-5p	0.28815
mmu-miR-298-5p	0.171883	mmu-miR-708-3p	0.256667	mmu-miR-143-3p	0.389059
mmu-miR-376a-3p	0.221935	mmu-miR-320-3p	0.33144	mmu-miR-652-3p	0.475185
mmu-miR-342-3p	0.362724	mmu-miR-22-3p	0.325647	mmu-miR-328-3p	0.41422
mmu-miR-30d-5p	0.419268	mmu-miR-195a-5p	0.288666	mmu-miR-154-5p	0.41497

blocks and mounted on clean, non-contaminated SuperFrost/Plus slides. The samples were

air dried for 2 h. The sections were then fixed in 4% paraformaldehyde/PBS (pH 7.2) at 4 °C for

## miRNAs and miRNA-9 in ALS

**Table 3.** miRNAs upregulated by more than twofold at 108 d

Name	Fold change	Name	Fold change	Name	Fold change
mmu-miR-34c-3p	2.021835	mmu-miR-26b-5p	3.34617	mmu-miR-376a-3p	3.44564
mmu-miR-3068-5p	2.904925	mmu-miR-125a-5p	2.090313	mmu-miR-342-3p	11.08121
mmu-miR-665-3p	2.030384	mmu-miR-101b-3p	2.550437	mmu-miR-219-5p	5.073216
mmu-miR-151-5p	2.602618	mmu-miR-369-3p	2.406828	mmu-let-7d-5p	4.153295
mmu-miR-465a-5p	2.359133	mmu-miR-128-3p	9.513007	mmu-miR-155-3p	2.426607
mmu-miR-136-3p	2.516482	mmu-miR-148b-3p	4.393795	mmu-miR-34b-5p	4.448474
mmu-miR-10a-5p	2.711264	mmu-miR-33-5p	2.026692	mmu-miR-434-5p	2.278956
mmu-miR-181a-5p	4.833038	mmu-miR-30c-5p	2.643801	mmu-miR-101a-3p	2.115394
mmu-miR-30a-5p	4.727729	mmu-miR-708-5p	2.341402	mmu-miR-140-5p	6.475232
mmu-miR-151-3p	2.453423	mmu-miR-1949	2.130279	mmu-miR-377-3p	3.186687
mmu-let-7g-5p	5.099158	mmu-miR-210-3p	2.678186	mmu-miR-382-3p	2.993366
mmu-miR-744-5p	3.089307	mmu-miR-5099	3.283915	mmu-miR-26a-5p	3.481209
mmu-miR-183-5p	2.439446	mmu-miR-98-5p	2.275855	mmu-miR-99a-5p	2.218298
mmu-miR-487b-3p	2.050231	mmu-miR-190a-5p	2.904538	mmu-miR-29c-3p	3.181396
mmu-miR-101a-3p	4.40404	mmu-miR-335-5p	3.390922	mmu-miR-320-3p	2.008822
mmu-miR-1224-5p	2.698565	mmu-miR-127-3p	2.198304	mmu-let-7i-5p	2.472667
mmu-miR-299a-3p	2.703685	mmu-miR-384-3p	4.501741	mmu-miR-126-3p	7.362062
mmu-miR-326-3p	2.084344	mmu-miR-181a-1-3p	2.095356	mmu-miR-195a-5p	3.209104
mmu-miR-5112	2.420771	mmu-miR-192-5p	2.014765	mmu-miR-29a-3p	3.794807
mmu-miR-132-3p	3.406183	mmu-miR-9-5p	3.190483	mmu-miR-376b-3p	3.904807
mmu-miR-23a-3p	4.193261	mmu-miR-137-3p	13.387	mmu-miR-21a-5p	2.047187
mmu-miR-139-5p	2.806742	mmu-miR-344b-3p	3.249742	mmu-miR-344d-3p	2.494471
mmu-let-7d-3p	3.009084				

**Table 4.** miRNAs downregulated by more than twofold at 108 d

Name	Fold change	Name	Fold change	Name	Fold change
mmu-miR-711	0.420725	mmu-miR-718	0.474571	mmu-miR-3092-3p	0.311307
mmu-miR-149-5p	0.492498	mmu-miR-3102-3p.2-3p	0.436533	mmu-miR-3072-5p	0.363899
mmu-miR-543-5p	0.390038	mmu-miR-5103	0.387455	mmu-miR-3473c	0.486902
mmu-miR-1247-5p	0.450099	mmu-miR-27a-5p	0.483725	mmu-miR-5119	0.346658
mmu-miR-210-5p	0.47395	mmu-miR-204-5p	0.448887	mmu-miR-223-3p	0.463509
mmu-miR-5109	0.462526	mmu-miR-292-5p	0.498894	mmu-miR-710	0.487984
mmu-miR-302a-3p	0.398372	mmu-miR-1927	0.450318	mmu-miR-883a-5p	0.455241
mmu-miR-3067-5p	0.438496	mmu-miR-320-5p	0.458729	mmu-miR-3067-3p	0.272833
mmu-miR-466c-5p	0.499798	mmu-miR-196a-2-3p	0.495296	mmu-miR-34a-5p	0.345214
mmu-miR-21a-3p	0.478556	mmu-miR-671-5p	0.403675	mmu-miR-3059-5p	0.497316
mmu-miR-804	0.461477	mmu-miR-3085-3p	0.480417	mmu-miR-664-3p	0.489577
mmu-miR-296-5p	0.475431	mmu-miR-3110-5p	0.413173	mmu-miR-684	0.297214
mmu-miR-20b-5p	0.476646	mmu-miR-874-5p	0.48141	mmu-miR-20a-5p	0.414289
mmu-miR-18b-3p	0.390485	mmu-miR-433-3p	0.465635	mmu-miR-674-3p	0.392879
mmu-miR-1306-5p	0.447726	mmu-miR-344i	0.490352	mmu-miR-10b-3p	0.478392
mmu-miR-5620-3p	0.406891	mmu-miR-764-5p	0.260616	mmu-miR-877-3p	0.354168
mmu-miR-5131	0.291022	mmu-miR-127-5p	0.359889	mmu-miR-701-5p	0.37725
mmu-miR-351-5p	0.480091	mmu-miR-193b-3p	0.440898	mmu-miR-683	0.491099
mmu-miR-3066-3p	0.476217	mmu-let-7f-5p	0.456079	mmu-miR-1907	0.44802
mmu-miR-496a-5p	0.351145	mmu-miR-547-3p	0.25347	mmu-miR-1224-3p	0.459508

## miRNAs and miRNA-9 in ALS

mmu-miR-1188-3p	0.456196	mmu-miR-3086-5p	0.254644	mmu-miR-3105-5p	0.37575
mmu-miR-324-3p	0.440787	mmu-miR-3092-5p	0.355693	mmu-miR-449c-3p	0.431572
mmu-miR-1193-3p	0.396077	mmu-miR-3544-3p	0.496269		

**Table 5.** miRNAs upregulated by more than twofold at 122 d

Name	Fold change	Name	Fold change	Name	Fold change
mmu-miR-711	2.32896	mmu-miR-678	3.872368	mmu-miR-377-3p	179.3738
mmu-miR-31-5p	2.533274	mmu-miR-669g	4.480121	mmu-miR-382-3p	2.885197
mmu-miR-103-3p	5.285574	mmu-miR-670-5p	4.910772	mmu-miR-26a-5p	3.440347
mmu-miR-1198-5p	2.528653	mmu-miR-467d-3p	5.19185	mmu-miR-374c-3p	2.945379
mmu-miR-1961	30.98079	mmu-miR-145a-3p	2.526941	mmu-miR-3081-5p	3.50498
mmu-miR-27b-3p	18.45688	mmu-miR-1949	3.034497	mmu-miR-296-3p	2.526625
mmu-miR-3066-5p	2.31918	mmu-miR-2861	3.601861	mmu-miR-467b-3p	3.343922
mmu-miR-96-3p	6.419321	mmu-miR-153-5p	7.510829	mmu-miR-3968	2.904469
mmu-miR-210-5p	7.216136	mmu-miR-1251-3p	7.230803	mmu-miR-5616-3p	5.676448
mmu-miR-350-3p	4.543493	mmu-miR-3091-3p	6.118372	mmu-miR-125a-3p	2.911635
mmu-miR-138-1-3p	4.547348	mmu-miR-3086-3p	3.337121	mmu-miR-466a-5p	2.196768
mmu-miR-5109	2.051979	mmu-miR-344e-3p	2.026537	mmu-let-7i-5p	3.376316
mmu-miR-10a-3p	6.047581	mmu-miR-709	3.271662	mmu-miR-505-5p	2.68932
mmu-miR-665-3p	2.318655	mmu-miR-3096b-5p	6.94822	mmu-miR-465c-5p	2.829785
mmu-miR-465a-5p	6.432397	mmu-miR-5099	2.541044	mmu-miR-206-3p	3.862473
mmu-miR-218-5p	4.521491	mmu-miR-467e-5p	2.55806	mmu-miR-99b-3p	3.148833
mmu-miR-695	3.717158	mmu-miR-98-5p	13.226	mmu-miR-1899	2.613095
mmu-miR-688	2.885817	mmu-miR-221-3p	2.531232	mmu-let-7c-5p	9.061984
mmu-miR-291b-3p	4.303074	mmu-miR-212-3p	2.484969	mmu-let-7e-5p	3.516478
mmu-let-7b-3p	6.085008	mmu-miR-130b-3p	6.847116	mmu-miR-3095-3p	5.609635
mmu-miR-3082-5p	2.352138	mmu-miR-200c-5p	5.341375	mmu-miR-3064-5p	45.63883
mmu-miR-5117-3p	2.985543	mmu-miR-423-3p	2.894901	mmu-miR-216b-3p	2.45094
mmu-miR-5616-5p	3.482754	mmu-miR-466d-5p	2.605069	mmu-miR-29a-3p	5.427003
mmu-miR-293-3p	8.437394	mmu-miR-668-5p	13.64906	mmu-miR-5107-5p	6.240363
mmu-miR-466c-5p	2.126331	mmu-miR-466n-3p	3.143261	mmu-miR-686	3.791119
mmu-miR-574-5p	3.488874	mmu-miR-467b-5p	7.416311	mmu-miR-693-5p	2.720883
mmu-miR-292-3p	4.438217	mmu-miR-5624-5p	4.839843	mmu-miR-375-3p	2.614048
mmu-miR-181a-5p	13.3904	mmu-miR-3963	2.914163	mmu-miR-3544-3p	15.35104
mmu-miR-466e-5p	5.671098	mmu-miR-425-3p	5.801479	mmu-miR-30c-1-3p	3.532289
mmu-miR-130a-3p	57.04854	mmu-miR-540-5p	4.883808	mmu-miR-378b	3.299737
mmu-miR-804	14.94782	mmu-miR-107-3p	5.57924	mmu-miR-3970	3.227847
mmu-miR-1953	5.237508	mmu-miR-122-3p	2.114285	mmu-miR-343	7.173264
mmu-miR-30a-5p	6.722681	mmu-miR-1892	7.617978	mmu-miR-712-5p	23.03883
mmu-miR-541-3p	3.076973	mmu-miR-1904	2.246417	mmu-miR-877-5p	5.172372
mmu-miR-216a-3p	4.261151	mmu-miR-137-3p	8.806756	mmu-miR-376b-3p	4.331379
mmu-miR-344c-5p	4.25928	mmu-miR-214-5p	3.644928	mmu-miR-710	6.820602
mmu-miR-532-3p	2.731047	mmu-miR-467c-3p	2.159236	mmu-let-7a-5p	19.70974
mmu-miR-5115	4.134992	mmu-miR-3060-5p	2.742718	mmu-miR-21a-5p	7.871505
mmu-miR-5120	5.739049	mmu-miR-1b-3p	4.869725	mmu-miR-301a-5p	6.460626
mmu-miR-679-5p	2.444481	mmu-miR-27a-5p	37.60953	mmu-miR-539-3p	2.589723
mmu-miR-27a-3p	123.1872	mmu-miR-410-3p	17.4879	mmu-miR-488-3p	2.507628
mmu-miR-136-5p	12.56823	mmu-miR-148b-5p	4.865344	mmu-miR-184-5p	2.007527

## miRNAs and miRNA-9 in ALS

mmu-miR-183-5p	2.440657	mmu-miR-204-5p	10.10235	mmu-miR-697	3.568439
mmu-miR-29b-3p	26.68454	mmu-miR-742-3p	6.462112	mmu-miR-181b-5p	3.519909
mmu-miR-2136	23.82247	mmu-miR-219-5p	58.88691	mmu-miR-145a-5p	3.35676
mmu-miR-299a-3p	8.800208	mmu-miR-25-5p	3.688824	mmu-miR-362-3p	2.638234
mmu-miR-3474	2.005535	mmu-miR-713	4.168932	mmu-miR-20a-5p	8.967211
mmu-miR-133b-5p	77.61893	mmu-let-7d-5p	6.013307	mmu-miR-491-3p	3.594207
mmu-miR-714	9.375649	mmu-miR-344-5p	2.514492	mmu-miR-880-5p	10.76771
mmu-miR-5105	2.236839	mmu-miR-466a-5p	12.01022	mmu-miR-221-5p	2.914677
mmu-miR-5112	27.06149	mmu-miR-346-3p	6.306549	mmu-miR-338-3p	56.80957
mmu-miR-204-3p	2.780989	mmu-miR-3095-5p	3.169364	mmu-miR-325-5p	2.283128
mmu-miR-1895	2.540623	mmu-miR-5114	7.031087	mmu-miR-691	3.144771
mmu-miR-26b-5p	2.114402	mmu-miR-183-3p	6.621648	mmu-miR-196b-3p	3.309794
mmu-miR-3065-3p	4.03445	mmu-miR-669h-3p	3.024023	mmu-miR-3070b-3p	2.775335
mmu-miR-494-5p	2.356306	mmu-miR-331-5p	4.581953	mmu-miR-194-2-3p	18.43107
mmu-miR-106a-5p	65.00243	mmu-miR-677-5p	3.246786	mmu-miR-188-5p	54.30583
mmu-miR-128-3p	12.73167	mmu-miR-195a-3p	2.184063	mmu-miR-147-3p	4.566976
mmu-miR-761	9.989739	mmu-miR-463-3p	12.53996	mmu-miR-5624-3p	2.644001
mmu-miR-883b-5p	2.35211	mmu-miR-1957a	11.74711	mmu-miR-346-5p	4.163306
mmu-miR-542-3p	7.764003	mmu-miR-1894-3p	31.13534	mmu-miR-30b-3p	2.051475
mmu-miR-1958	6.32935	mmu-miR-1971	6.442928	mmu-miR-701-5p	5.823002
mmu-miR-1893	3.991812	mmu-miR-671-5p	10.50069	mmu-miR-28a-3p	7.908172
mmu-miR-466b-5p	3.301444	mmu-miR-499-3p	172.2427	mmu-miR-1907	5.036028
mmu-miR-7a-2-3p	2.046015	mmu-miR-107-5p	5.46512	mmu-miR-3105-5p	2.774986
mmu-miR-466m-5p	23.50902	mmu-miR-665-5p	3.522869	mmu-miR-489-5p	6.494757
mmu-miR-5625-3p	3.090129	mmu-miR-503-5p	3.001966	mmu-miR-5621-5p	8.468883
mmu-miR-29b-1-5p	3.860122	mmu-miR-140-5p	3.422258		
mmu-miR-743b-5p	10.07274	mmu-miR-142-3p	222.1103		

10 min, digested with proteinase K (Roche Diagnostics) at 10 µg/mL at 37 °C for 10 min, acetylated for 10 min, and dehydrated in fresh gradient ethanol solutions. The hybridization mixture was heated (probe final concentration: 25 nM) at 65 °C for 5 min and chilled on ice. The sections were applied with 5 µl of hybridization mix, hybridized overnight 53 °C, and covered with Nescofilm in a humidified chamber with 50% formamide, 1× SSC. The cover slips were removed from 5× SSC at room temperature (RT). The sections were washed twice for 30 min at 53 °C in 50% formamide and 0.1% Tween-20, 1× SSC. The sections were washed thrice for 15 min in 0.2× SSC and PBS at RT. The sections were then blocked in blocking solution with 10% heat-inactivated goat serum and 0.1% Tween-20 for 1 h at RT and finally incubated for 1.5 h at RT in anti-dioxygenine antibody (anti-DIG-PA Fab fragments, Roche Diagnostics) diluted to 1:800 with the blocking solution. After the sample was washed twice for 20 min with 0.1% Tween-20 in PBS, phos-

phatase activity was determined using nitro blue tetrazolium chloride/5-bromo-4-chloro-3-indolyl phosphate p-toluidine as the stabilized solution (Eurobio) for 5 h. The sections were finally mounted with 80% glycerol.

### Statistical analysis

Data are presented as the mean ± standard deviation (SD). The homogeneity of variance was performed using SPSS 13.0 software. Independent sample t-tests were performed when normality and equality of variance were observed to compare the differences in miRNA-9 between ALS and wild-type mice. The significant level was defined as  $p < 0.05$ .

### Results

#### *Differential expression of miRNAs between the G93A-SOD1 transgenic mice and the wild-type mice*

Among the 1227 detected miRNAs, 45, 67, and 205 miRNAs were upregulated by twofold and

## miRNAs and miRNA-9 in ALS

**Table 6.** miRNAs downregulated by more than twofold at 122 d

Name	Fold change	Name	Fold change	Name	Fold change
mmu-miR-495-5p	0.339321	mmu-miR-190a-5p	0.193533	mmu-miR-874-5p	0.398086
mmu-miR-3068-5p	0.247305	mmu-miR-10b-5p	0.266441	mmu-miR-3069-3p	0.361669
mmu-miR-290-3p	0.252711	mmu-miR-338-5p	0.138908	mmu-miR-652-5p	0.42407
mmu-miR-1843b-3p	0.37422	mmu-miR-135a-5p	0.24666	mmu-miR-433-3p	0.186811
mmu-miR-151-5p	0.453855	mmu-miR-712-3p	0.286408	mmu-miR-1843a-5p	0.378559
mmu-miR-291a-5p	0.38995	mmu-miR-127-3p	0.419585	mmu-miR-193b-3p	0.432846
mmu-miR-29a-5p	0.444011	mmu-miR-324-3p	0.320562	mmu-miR-7a-5p	0.473021
mmu-miR-3084-3p	0.106545	mmu-miR-138-5p	0.283583	mmu-miR-331-3p	0.346048
mmu-miR-28a-5p	0.311724	mmu-miR-144-3p	0.125605	mmu-miR-375-5p	0.340044
mmu-miR-361-5p	0.467213	mmu-miR-718	0.454415	mmu-miR-3072-5p	0.14226
mmu-miR-196a-1-3p	0.368253	mmu-let-7i-3p	0.377898	mmu-miR-3473c	0.350358
mmu-miR-296-5p	0.23509	mmu-miR-3102-3p.2-3p	0.246599	mmu-miR-451a	0.348975
mmu-let-7g-5p	0.347148	mmu-miR-3098-3p	0.350802	mmu-miR-483-3p	0.396762
mmu-miR-744-5p	0.164894	mmu-miR-370-3p	0.316776	mmu-miR-34a-5p	0.157207
mmu-miR-146b-5p	0.321076	mmu-miR-5103	0.253431	mmu-miR-3059-5p	0.293724
mmu-miR-325-3p	0.361389	mmu-miR-298-5p	0.330357	mmu-miR-3971	0.388255
mmu-miR-487b-3p	0.318543	mmu-miR-376a-3p	0.104594	mmu-miR-873a-5p	0.355127
mmu-miR-101a-3p	0.189311	mmu-miR-30d-5p	0.322125	mmu-miR-1943-3p	0.368966
mmu-miR-1224-5p	0.360472	mmu-miR-193a-3p	0.297904	mmu-miR-3475	0.238778
mmu-miR-431-5p	0.474967	mmu-miR-186-5p	0.460699	mmu-miR-3104-3p	0.280163
mmu-miR-615-5p	0.35682	mmu-miR-543-3p	0.282108	mmu-miR-92a-3p	0.493385
mmu-miR-3105-3p	0.422037	mmu-miR-411-3p	0.250887	mmu-miR-467a-5p	0.136188
mmu-miR-326-3p	0.394951	mmu-miR-155-3p	0.396201	mmu-miR-674-3p	0.487958
mmu-miR-23a-3p	0.461305	mmu-miR-5626-5p	0.33411	mmu-miR-125b-2-3p	0.254925
mmu-miR-340-5p	0.339629	mmu-miR-379-5p	0.288851	mmu-miR-10b-3p	0.211123
mmu-miR-34c-5p	0.074025	mmu-miR-153-3p	0.37579	mmu-miR-185-5p	0.357345
mmu-miR-139-5p	0.353424	mmu-miR-129-5p	0.469387	mmu-miR-143-3p	0.162113
mmu-let-7d-3p	0.362006	mmu-miR-3069-5p	0.430008	mmu-miR-652-3p	0.256424
mmu-miR-382-5p	0.19934	mmu-miR-1843b-5p	0.44958	mmu-miR-328-3p	0.347203
mmu-miR-491-5p	0.368848	mmu-miR-219-2-3p	0.243031	mmu-miR-541-5p	0.280503
mmu-miR-1843a-3p	0.130198	mmu-miR-3072-3p	0.372183	mmu-miR-379-3p	0.373429
mmu-miR-101b-3p	0.163835	mmu-miR-383-5p	0.393393	mmu-miR-9-3p	0.214284
mmu-miR-369-3p	0.49817	mmu-miR-3085-3p	0.241654	mmu-miR-324-5p	0.189889
mmu-miR-341-3p	0.444242	mmu-miR-5621-3p	0.2397	mmu-miR-741-3p	0.329126
mmu-miR-148b-3p	0.483882	mmu-miR-708-3p	0.195404	mmu-miR-154-5p	0.372162
mmu-miR-182-5p	0.289559	mmu-miR-320-3p	0.415748	mmu-miR-551b-3p	0.322774
mmu-miR-3107-5p	0.367641	mmu-miR-22-3p	0.384327	mmu-miR-329-5p	0.452029
mmu-miR-210-3p	0.305306	mmu-miR-195a-5p	0.262231	mmu-miR-361-3p	0.345876
mmu-miR-132-5p	0.366162	mmu-miR-3110-5p	0.267735		

78, 68, and 116 miRNAs were downregulated by twofold in the ALS transgenic mice than in the wild-type mice at 95, 108, and 122 d, respectively (**Tables 1-6**).

Among the differentially expressed miRNAs, miRNA-9 is highly expressed in the nervous system. miRNA-9 is involved in proliferation and

differentiation of neural stem cells (NSCs). In the G93A-SOD1 transgenic mice, expression changes in NSCs were detected. Therefore, miRNA-9 was chosen as the investigation target. Microarray results showed that miRNA-9 was upregulated at the three time points. Heat map and hierarchical clustering analysis showed a clear distinction between the trans-

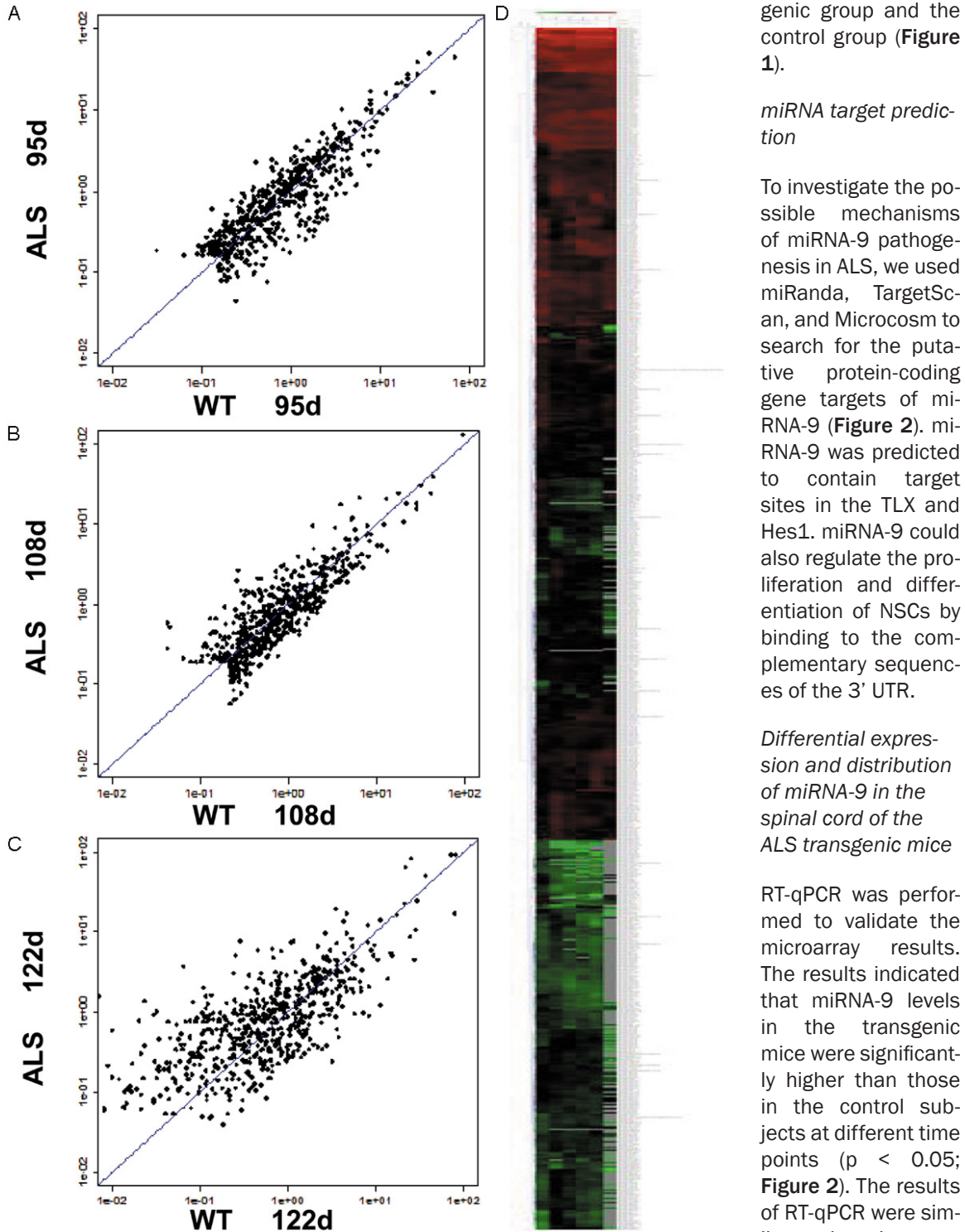


**Figure 1.** Differential expression of miRNAs in the spinal cord of ALS and wild-type mice. A-C: Scatter plots of expressed miRNAs at 95, 108, and 122 d, respectively. D: Heat map and hierarchical clustering. The heat map diagram shows the result of the two-way hierarchical clustering of miRNAs. Each row represents an miRNA and each column represents a sample. The miRNA clustering tree is shown on the left and the sample clustering tree is shown on top. The color scale shown at the top illustrates the relative expression level of an miRNA in a specific slide: red represents a relatively high expression level; green represents relatively low expression levels.

genic group and the control group (**Figure 1**).

#### *miRNA target prediction*

To investigate the possible mechanisms of miRNA-9 pathogenesis in ALS, we used miRanda, TargetScan, and Microcosm to search for the putative protein-coding gene targets of miRNA-9 (**Figure 2**). miRNA-9 was predicted to contain target sites in the TLX and Hes1. miRNA-9 could also regulate the proliferation and differentiation of NSCs by binding to the complementary sequences of the 3' UTR.

#### *Differential expression and distribution of miRNA-9 in the spinal cord of the ALS transgenic mice*

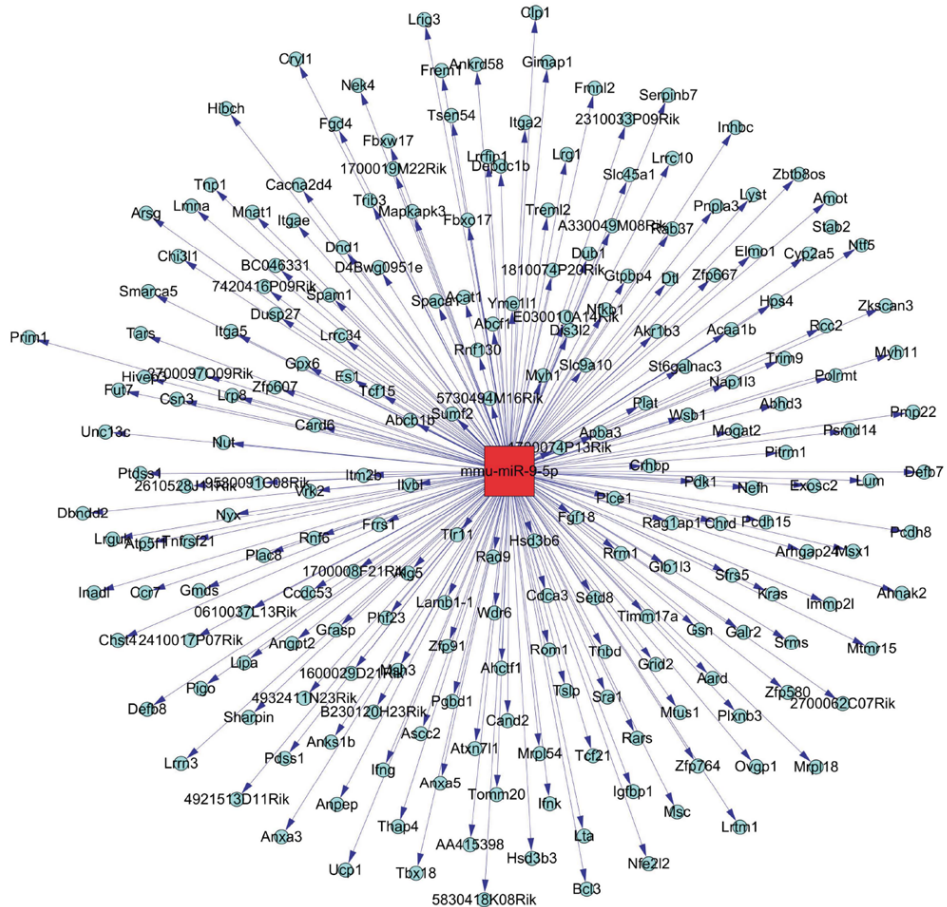
RT-qPCR was performed to validate the microarray results. The results indicated that miRNA-9 levels in the transgenic mice were significantly higher than those in the control subjects at different time points ( $p < 0.05$ ; **Figure 2**). The results of RT-qPCR were similar to the microarray results.

In-situ hybridization was performed to investigate the distribution of miRNA-9 in the spinal cord. The



# miRNAs and miRNA-9 in ALS

A



B

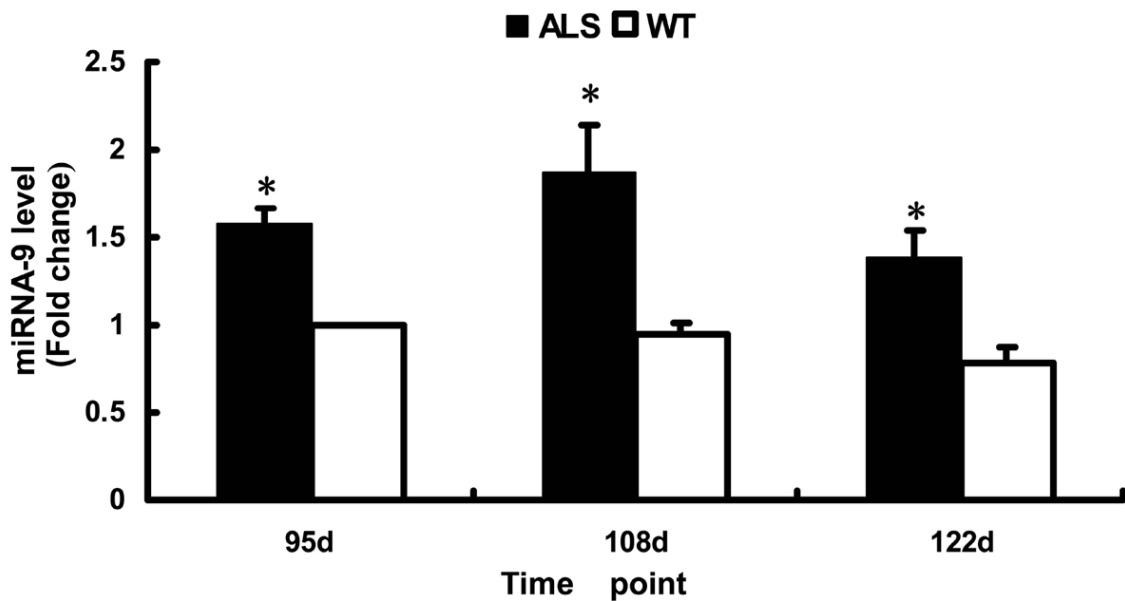


**Figure 2.** A: Network of miRNA-9 regulatory genes. B: Expression of miRNA-9 in the spinal cord of ALS and wild-type mice. Results of RT-qPCR indicate that the expression of miRNA-9 was upregulated (n = 3). \*p < 0.05 vs. wild-type littermates.

results indicated that miRNA-9 was localized in the cytoplasm of the positive cells. The miRNA-

9-positive cells were mainly detected in the gray matter of the ventral horn and the dorsal

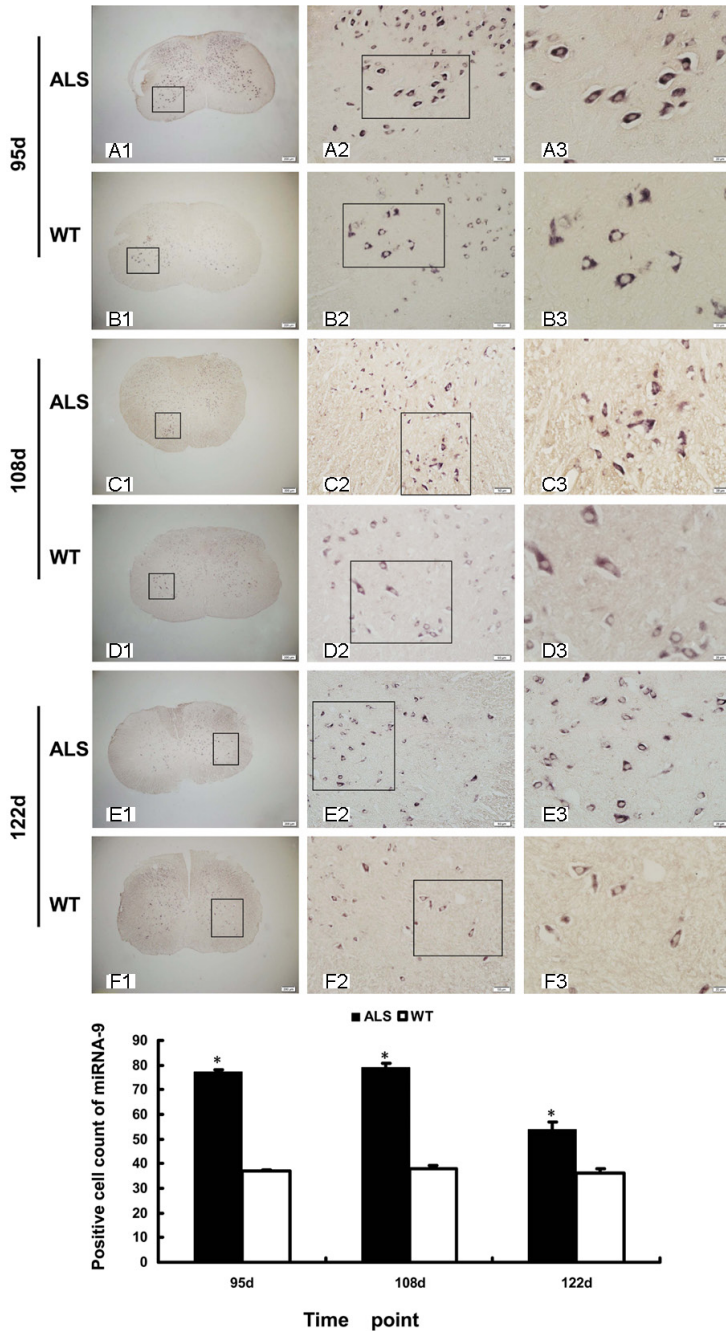


**Figure 3.** Expression and cellular distribution of miRNA-9 in the spinal cord of ALS and wild-type mice. Results of ISH show that the miRNA-9-positive cells were mainly detected in the gray matter of the ventral horn and the dorsal horn of the spinal cord. The majority of the miRNA-9-positive cells were located in the ventral horn of the gray matter. A1-A3: Represent the distribution of miRNA-9-positive cells in the ALS mice at 95 d. B1-B3: Represent the distribution of miRNA-9-positive cells in the WT mice at 95 d. C1-C3: Represent the distribution of miRNA-9-positive cells in the ALS mice at 108 d. D1-D3: Represent the distribution of miRNA-9-positive cells in the WT mice at 108 d. E1-E3: Represent the distribution of miRNA-9-positive cells in the ALS mice at 122 d. F1-F3: Represent the distribution of miRNA-9-positive cells in the WT mice at 122 d. Scale bar = 200, 50, 20  $\mu$ m. The total number of miRNA-9-positive cells was counted (n = 3). \*p < 0.05 vs. wild-type littermates.

horn of the spinal cord in ALS and wild-type mice at different time points. The majority of the miRNA-9-positive cells were located in the ventral horn of the gray matter, the locus of neurodegeneration. The number of miRNA-9-positive cells was significantly increased at post-natal 95, 108, and 122 d in the ALS mice compared with the wild-type mice (p < 0.05; **Figure 3**).

In addition to injury on the motor neurons in the spinal cord, injury on the motor neurons in the brain can occur in ALS, in which muscle atrophy and paralysis possibly occur. Therefore, the expression of miRNA-9 was also detected in the brain and the gastrocnemius. miRNA-9-positive cells were also detected in the cerebral cortex and the hippocampi but were not found in the gastrocnemius (data not shown).

**Discussion**

miRNAs have an important function in many cellular processes. miRNAs can interact with specific sequences of target mRNA (mainly in the 3' UTR), recruiting the RNA-induced silencing complex (RISC). On the basis of complete or incomplete miRNA-mRNA complementation, miRNAs can lead to degradation or translational suppression of target mRNA [11]. Therefore, miRNAs are a part of a novel regulatory pathway [12].

Early studies on the development of the nervous system evaluated the consequences of the decrease in the Dicer gene (which results in the absence of mature miRNAs) during neurogenesis. In zebrafish, the complete absence of Dicer leads to critical defects in the general morphology of the central nervous system and the peripheral nervous system; neuronal differentiation is also im-

paired [13]. miRNAs also have an important function in the pathogenesis of neurodegenerative diseases such as Alzheimer's [14], Parkinson's [15], and Huntington's diseases [16]. In ALS, a few studies on miRNAs have been reported. miRNA-206, a skeletal muscle-specific miRNA, delays the progression of ALS and promotes the regeneration of the neuromuscular synapses in mice [17]. In the present study, microarray results showed for the first time that numerous miRNAs were differentially expressed in the spinal cord at different time points in the G93A-SOD1 transgenic mice. The function of these differentially expressed miRNAs should be investigated in future studies.

miRNA-9 is highly expressed in the nervous system and conserved among species, exhibiting 100% similarity between *Drosophila melanogaster* and vertebrates [18]. Studies with different model systems have revealed that miRNA-9 regulates neurogenesis by acting on neural or non-neural cell lineages. For example, miRNA-9 suppresses the expression of TLX, an essential regulator of NSC self-renewal, and maintains the adult NSCs in an undifferentiated and self-renewable state, thereby regulating the proliferation and distribution of NSCs [19]. Increased miRNA-9 expression reduces the proliferation of the mouse NSCs and accelerates neural differentiation. Antisense knockdown of miRNA-9 leads to the proliferation of NSCs [20]. In addition, the overexpression of miRNA-9 decreases the levels of Hes1, which regulates proliferation and differentiation characteristics of NSCs. The overexpression of miRNA-9 also promotes cell cycle exit and neuronal differentiation. By contrast, the knockdown of miRNA-9 inhibits neuronal differentiation [21]. miRNA-9 can promote the neural differentiation of MSCs in the bone marrow by targeting Zfp521Z [22]. The loss of miRNA-9 suppresses proliferation but promotes the migration of hNPCs cultured in vitro [23]. These findings have indicated that miRNA-9 may regulate neural differentiation.

In ALS, the proliferation and differentiation of NSCs and neural progenitor cells (NPCs) have been debated. Previous studies demonstrated that an increase in the proliferation of NPCs is observed in the ependymal zone surrounding the central canal (EZ) in the spinal cord; increased de novo neurogenesis from NPCs is also observed during ALS-like disease onset

and progression [24]. In another study, NSCs are intravenously engrafted in the central nervous system of ALS-affected animals and their wild-type counterparts, resulting in a higher cell grafting efficiency in the ALS animals than in the wild-type animals; the two main fates observed in these animals are neuronal and astrocytic [25]. In SOD1G93AG1H mice, the number of nestin-positive NPCs is greatly increased, the majority of nestin-positive NPCs co-expresses the astrocyte marker GFAP, and a small number of GFAP co-expresses the neuronal marker NeuN [26]. In wobbler mouse, the percentage of neurons obtained from in vitro differentiation of NPCs is significantly higher than that from the healthy mice [27].

Our results indicated that miRNA-9 levels were upregulated at 95, 108, and 122 d in the G93A-SOD1 transgenic mice compared with the control mice. The miRNA-9-positive cells were detected in the ventral horn and the dorsal horn of the spinal cord. The majority of miRNA-9-positive cells were located in the ventral horn of the spinal cord, the locus of neurodegeneration. However, the function of miRNA-9 as a regulator in the differentiation of NSCs and NPCs in ALS remains unclear. The increase in expression and the distribution characteristics of miRNA-9 may be involved in the differentiation of the neurons derived from NSCs and NPCs in ALS.

ALS is the third most common neurodegenerative disease occurring in adulthood (after Alzheimer's and Parkinson's diseases). To date, no effective therapies are available for patients with ALS. The transplantation of the NSCs derived from the central nervous system is a promising therapeutic strategy to treat ALS [28]. The directional differentiation of the NSCs into neurons should be determined and could promote effective treatment. Therefore, the regulatory mechanisms of miRNAs in the proliferation and differentiation of the NSCs should be elucidated to provide a new treatment method.

### Acknowledgements

The microarray experiments were performed by KangChen Bio-tech, Shanghai, China. This study was supported by the National Natural Science Foundation of China (Grant No. 81271413), the Shandong Province Science

and Technology Development Program of China (Grant No. 2012GSF11827), the Shandong Province Natural Science Foundation of China (Grant No. ZR2012HQ021), the Muscular Dystrophy Association (Grant Nos. 157511 and 254530), the ALS Therapy Alliance (Grant No. 2013D001622), the Shandong Province Taishan Scholar Project, and the Shandong Province Education Department of China (Grant Nos. J12LK51 and J11LF16).

#### Disclosure of conflict of interest

None.

**Address correspondence to:** Dr. Yingjun Guan, Department of Histology and Embryology, Weifang Medical University, Shandong 261053, China. Fax: 86-0536-8271216; E-mail: guanyj@wfmuc.edu.cn; Dr. Xin Wang, Department of Neurosurgery, BL141 and LMRC 111, Brigham and Women's Hospital, Harvard Medical School, Boston, Massachusetts, 02115, USA. Fax: +1 617-278-6937; E-mail: xwang@rics.bwh.harvard.edu

#### References

- [1] Lagos-Quintana M, Rauhut R, Lendeckel W, Tuschl T. Identification of novel genes coding for small expressed RNAs. *Science* 2001; 294: 853-858.
- [2] Wei J, Wang F, Kong LY, Xu S, Doucette T, Ferguson SD, Yang Y, McEnery K, Jethwa K, Gijshi O, Qiao W, Levine NB, Lang FF, Rao G, Fuller GN, Calin GA, Heimberger AB. miR-124 inhibits STAT3 signaling to enhance T cell-mediated immune clearance of glioma. *Cancer Res* 2013; 73: 3913-26.
- [3] Chi L, Gan L, Luo C, Lien L, Liu R. Temporal Response of Neural Progenitor Cells to Disease Onset and Progression in Amyotrophic Lateral Sclerosis-Like Transgenic Mice. *Stem Cells Dev* 2007; 16: 579-88.
- [4] Kulshreshtha D, Vijayalakshmi K, Alladi PA, Sathyaprabha TN, Nalini A, Raju TR. Vascular Endothelial Growth Factor Attenuates Neurodegenerative Changes in the NSC-34 Motor Neuron Cell Line Induced by Cerebrospinal Fluid of Sporadic Amyotrophic Lateral Sclerosis Patients. *Neurodegener Dis* 2011; 8: 322-30.
- [5] Griffiths-Jones S, Grocock RJ, van Dongen S, Bateman A, Enright AJ. miRBase: microRNA sequences, targets and gene nomenclature. *Nucleic Acids Res* 2006; 34: D140-4.
- [6] Flynt AS, Lai EC. Biological principles of microRNA-mediated regulation: shared themes amid diversity. *Nat Rev Genet* 2008; 9: 831-42.
- [7] De Pietri Tonelli D, Pulvers JN, Haffner C, Murchison EP, Hannon GJ, Huttner WB. miRNAs are essential for survival and differentiation of newborn neurons but not for expansion of neural progenitors during early neurogenesis in the mouse embryonic neocortex. *Development* 2008; 135: 3911-21.
- [8] Wong HK, Veremeyko T, Patel N, Lemere CA, Walsh DM, Esau C, Vanderburg C, Krichevsky AM. De-repression of FOXO3a death axis by microRNA-132 and -212 causes neuronal apoptosis in Alzheimer's disease. *Hum Mol Genet* 2013; 22: 3077-92.
- [9] Sibley CR, Seow Y, Curtis H, Weinberg MS, Wood MJ. Silencing of Parkinson's disease-associated genes with artificial mirtron mimics of miR-1224. *Nucleic Acids Res* 2012; 40: 9863-9875.
- [10] Chen Y, Guan Y, Liu H, Wu X, Yu L, Wang S, Zhao C, Du H, Wang X. Activation of the Wnt/beta-catenin signaling pathway is associated with glial proliferation in the adult spinal cord of ALS transgenic mice. *Biochem Biophys Res Commun* 2012; 420: 397-403.
- [11] Saugstad JA. MicroRNAs as effectors of brain function with roles in ischemia and injury, neuroprotection, and neurodegeneration. *J Cereb Blood Flow Metab* 2010; 30: 1564-76.
- [12] Smirnova L, Grafe A, Seiler A, Schumacher S, Nitsch R, Wulczyn FG. Regulation of miRNA expression during neural cell specification. *Eur J Neurosci* 2005; 21: 1469-77.
- [13] Giraldez AJ, Cinalli RM, Glasner ME, Enright AJ, Thomson JM, Baskerville S, Hammond SM, Bartel DP, Schier AF. MicroRNAs regulate brain morphogenesis in zebrafish. *Science* 2005; 308: 833-838.
- [14] Lukiw WJ. Micro-RNA speciation in fetal, adult and Alzheimer's disease hippocampus. *Neuroreport* 2007; 18: 297-300.
- [15] Wang G, van der Walt JM, Mayhew G, Li YJ, Zuchner S, Scott WK, Martin ER, Vance JM. Variation in the miRNA-433 binding site of FGF20 confers risk for Parkinson disease by overexpression of alpha-synuclein. *Am J Hum Genet* 2008; 82: 283-9.
- [16] Johnson R, Zucato C, Belyaev ND, Guest DJ, Cattaneo E, Buckley NJ. A microRNA-based gene dysregulation pathway in Huntington's disease. *Neurobiol Dis* 2008; 29: 438-45.
- [17] Williams AH, Valdez G, Moresi V, Qi X, McAnally J, Elliott JL, Bassel-Duby R, Sanes JR, Olson EN. MicroRNA-206 delays ALS progression and promotes regeneration of neuromuscular synapses in mice. *Science* 2009; 326: 1549-1554.
- [18] Lagos-Quintana M, Rauhut R, Yalcin A, Meyer J, Lendeckel W, Tuschl T. Identification of tissue-specific microRNAs from mouse. *Curr Biol* 2002; 12: 735-9.

## miRNAs and miRNA-9 in ALS

- [19] Shi Y, Chichung Lie D, Taupin P, Nakashima K, Ray J, Yu RT, Gage FH, Evans RM. Expression and function of orphan nuclear receptor TLX in adult neural stem cells. *Nature* 2004; 427: 78-83.
- [20] Zhao C, Sun G, Li S, Shi Y. A feedback regulatory loop involving microRNA-9 and nuclear receptor TLX in neural stem cell fate determination. *Nat Struct Mol Biol* 2009; 16: 365-71.
- [21] Tan SL, Ohtsuka T, Gonzalez A, Kageyama R. MicroRNA9 regulates neural stem cell differentiation by controlling Hes1 expression dynamics in the developing brain. *Genes Cells* 2012; 17: 952-61.
- [22] Han R, Kan Q, Sun Y, Wang S, Zhang G, Peng T, Jia Y. MiR-9 promotes the neural differentiation of mouse bone marrow mesenchymal stem cells via targeting zinc finger protein 521. *Neurosci Lett* 2012; 515: 147-52.
- [23] Delaloy C, Liu L, Lee JA, Su H, Shen F, Yang GY, Young WL, Ivey KN, Gao FB. MicroRNA-9 coordinates proliferation and migration of human embryonic stem cell-derived neural progenitors. *Cell Stem Cell* 2010; 6: 323-335.
- [24] Chi L, Ke Y, Luo C, Li B, Gozal D, Kalyanaraman B, Liu R. Motor neuron degeneration promotes neural progenitor cell proliferation, migration, and neurogenesis in the spinal cords of amyotrophic lateral sclerosis mice. *Stem Cells* 2006; 24: 34-43.
- [25] Mitrecic D, Nicaise C, Gajovic S, Pochet R. Distribution, differentiation, and survival of intravenously administered neural stem cells in a rat model of amyotrophic lateral sclerosis. *Cell Transplant* 2010; 19: 537-48.
- [26] Juan L, Dawei Z, Julie AD. Increased number and differentiation of neural precursor cells in the brainstem of superoxide dismutase 1(G93A) (G1H) transgenic mouse model of amyotrophic lateral sclerosis. *Neurol Res* 2007; 29: 204-9.
- [27] DiFebo F, Curti D, Botti F, Biella G, Bigini P, Mennini T, Toselli M. Neural precursors (NPCs) from adult L967Q mice display early commitment to "in vitro" neuronal differentiation and hyperexcitability. *Exp Neurol* 2012; 236: 307-18.
- [28] Pandya RS, Mao LL, Zhou EW, Bowser R, Zhu Z, Zhu Y, Wang X. Neuroprotection for amyotrophic lateral sclerosis: role of stem cells, growth factors, and gene therapy. *Cent Nerv Syst Agents Med Chem* 2012; 12: 15-27.